A Wavefront Launching Model for Predicting Channel Impulse Response

Michael Robinson

Syracuse Research Corporation
6225 Running Ridge Road
North Syracuse, NY 13212

Abstract − Maintaining the topology of an expanding wavefront surface allows for a simpler time-domain wave ray launching model that is free from the problems associated with ray catching. In addition to the usual ray location and direction information, the wavefront launching model stores which rays are adjacent in the advancing wavefront surface. The added information allows interpolation over this surface, so the model easily incorporates diffracted waves and power density changes from beam spreading.

I. INTRODUCTION

Ray tracing and launching methods have become popular for predicting wave propagation in complex geometries. Ray tracing methods trace "dominant" paths from source to receiver [1]. This can result in a large number of redundant rays being traced if the model has many receiver points. Ray launching reduces this computational burden by tracing a fixed number of rays from the source, which are followed as they scatter around the geometry. If they pass sufficiently close to a receiver point, they contribute to that receiver's response. This leads to the problem of "ray catching," where rays can be "double counted" at a receiver [2].

This paper describes a method of ray launching that avoids double counting by respecting the topological structure of the moving wavefront. Unlike ray catching, in which the wavefront is *extrapolated* to the receiver point, this method *interpolates* the wavefront to the receiver point. This avoids causing errors associated with extending the wavefront beyond its true extent. The topological information also allows accurate wavefront power densities to be computed purely from geometric considerations.

II. TOPOLOGICAL ASPECTS OF WAVEFRONT PROPAGATION

The aim of this paper is to present a method for computing the solution to the scalar wave equation in a region Ω, with a transmitted signal f,

$$\nabla^2 u - \frac{1}{c^2}\frac{\partial^2 u}{\partial t^2} = f(x,t),\ (x,t) \in \Omega \times \mathbb{R}^+ \quad (1)$$

where the parameter c describes the wave propagation speed, which depends on the medium in which the wave propagates [3]. This equation can be used to predict electromagnetic wave propagation where polarization is not expected to be an issue, or in small-amplitude acoustic settings. In the case of acoustic waves, u describes the pressure at a given point, while for electromagnetic waves, it describes a component of the electric field vector. Typical indoor or outdoor urban environments do not show marked differences in electromagnetic wave propagation due to polarization, so it is reasonable to choose a component of the electric field parallel to the radiating elements [4].

A. Waves in Unbounded Media

When the spatial domain Ω is of odd dimension, Huygen's principle ensures that there are well-defined wavefronts [3]. In an unbounded spatial domain, where $\Omega = \mathbb{R}^3$, this is apparent from the Green's function of equation (1),

$$G_u(x,\xi,t,\tau) = \frac{\delta(|x-\xi|-c(t-\tau))}{4\pi(|x-\xi|-c(t-\tau))}. \quad (2)$$

The locus of points where $G(x,\xi,t,\tau) \neq 0$ is called a "wavefront". In general, the "wavefront set" shall be defined as

$$W(\xi,\tau) = \left\{(x,t) \in \Omega \times \mathbb{R}^+ \,\middle|\, G(x,\xi,t,\tau) \neq 0\right\} \quad (3)$$

where G is the Green's function relevant to the particular spatial geometry Ω. In unbounded media, the wavefront set does not change topologically with time; it is always spherical.

B. Reflecting Half-Space

If an infinite, flat boundary is introduced, the method of images leads to a new Green's function for equation (1),

$$G_h(x,\xi,t,\tau) = G_u(x,\xi,t,\tau) - G_u(x,\xi',t,\tau) \quad (4)$$

where ξ' is the image of ξ reflected across the boundary. It is evident that the wavefront set of this Green's function does not undergo topological change. Like the unbounded case, it is always topologically equivalent to a sphere.

C. Diffraction and Topological Change

Diffraction causes the topology of the wavefront set to change in the vicinity of convex boundary edges. The wavefront set is no longer confined to a thin surface once diffraction occurs, due to dispersion. The Uniform Theory of Diffraction (UTD) predicts that diffracted wave power falls off like $t^{-3/2}$ at a given point (equation (16) of [5]). In light of this, it is reasonable to assume that the diffracted wave can be approximated by confining its power to the "leading edge" of the wavefront set. This removes the dispersive effects of diffraction, and makes diffracted waves easy to model with the wavefront approach. This approximation restricts the frequencies the model can accurately treat and introduces a small time delay error. Further, a scalar wave model ignores the polarization-dependent effects of electromagnetic wave diffraction. To mitigate these concerns, frequency- and polarization-specific diffraction coefficients must be chosen for the operating frequency and incident polarization. Alternatively, one may use empirical diffraction coefficients that explicitly ignore frequency, phase delay, and polarization [6].

Having motivated a non-dispersive scalar approximation for diffraction, we now look at how diffraction changes wavefront topology. Diffraction occurs when a wavefront crosses an edge in the boundary; wavefront points on one side of the edge are sent off at vastly different angles from those on the other side. The continuity of the wavefront is disrupted along such an edge, cutting the incident wavefront into two distinct pieces. This discontinuity is smoothed out by the introduction of a diffracted wave, as shown in Fig. 1. Using the UTD approximation, the edge begins to emit a diffracted wave when it is touched by an incident wavefront [5].
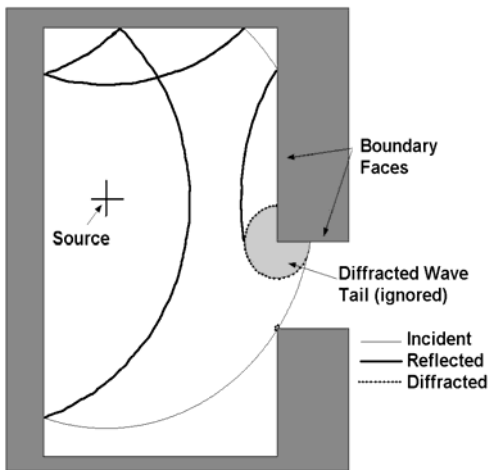

Fig. 1. An example of the topological changes of a wavefront: Waves near the left side of the room maintain their topology after being reflected at flat surfaces and concave corners. Waves at the convex corners (exit of the room) undergo a topology change as a distinct diffracted wave is created.

III. STORAGE OF TOPOLOGICAL INFORMATION

In the wavefront launching model, the wavefront set is sampled both in space and in time, resulting in a collection of discrete points. A unit vector representing the motion of the wavefront is tied to each of these points and fills the same role as rays do in ray tracing or launching models. The topology of the wavefront is represented by maintaining links between adjacent points both in space and in time. This allows new points or rays to be interpolated anywhere in the wavefront set.

A group of four wavefront points that form a link-connected loop in space is called a "patch". Two patches that are linked in the time dimension are called a "cube". (See Fig. 2) It is often of interest to know if a wavefront crosses a particular point in space x over a given interval of time $[t_0, t_1]$: that is, if x belongs to the set $W(\xi,\tau) \cap \Omega \times [t_0, t_1]$. This problem may be solved computationally by checking if the point of interest can be found in any of the wavefront's cubes that are valid on the time interval of interest. This eliminates the problem of ray-catching, since the wavefront is interpolated rather than extrapolated to the point. Further, the incident power density at any point on the patch is easy to calculate: the wave power at the four points on the patch is smoothly distributed over the surface of the patch.
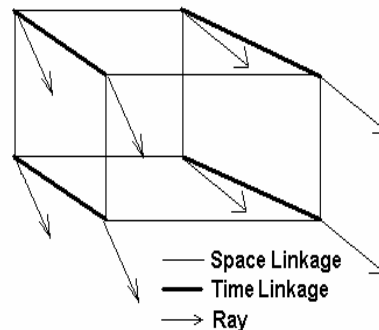

Fig. 2. Points, rays, and linkages of a "cube".

IV. PROPAGATION OF THE WAVEFRONT

The wavefront model generates the wavefront set by propagating snapshots of the wavefront at earlier times. It uses two previous snapshots (points, rays, and spatial linkages) W_{i-1} and W_i to generate a new one W_{i+1}, where each W_n is valid over $t \in [t_{n-1}, t_n]$. Where rays do not cross a diffracting edge, they are propagated according to the usual rules of ray tracing. (See, for example, [1] or [2])

When a point on the wavefront comes near a diffracting edge, the wavefront model checks to see if any of the cubes containing that point intersect the edge. If so, then a new diffracted wavefront will be launched from that edge. The incident wavefront's rays will be unaffected by

the diffracting edge, although the links of the incident wavefront will be broken along the edge.

The structure of the diffracted wave is created from the incident wave by decomposing the patches incident on the edge. It is important to realize that a diffracted wave develops as different patches of the incident wavefront cross the edge at different times. It is important to allow these patches to duplicate points and rays along the edges if there is no explicit topological linkage between them. That way, the diffracted wave can form over several time steps. (This is not the most memory efficient approach, but it is simple and fast.)

Once the patches for generating the diffracted wave are found, each one is used to create a family of diffracted wave patches. Since the diffracting edge generates the diffracted wave, the diffracted wave patches must be launched from that edge. The launch points are found by projecting each incident patch onto the edge. To simplify matters geometrically, the two points that are farthest apart are used as launch points for the diffracted patches. Then the rays are built by decomposing them into components. The ray component parallel to the edge is computed by projecting the incident ray onto the edge,

$$\frac{e \bullet v}{\|e\|^2} \tag{5}$$

where v is the incident ray, and e is parallel to the edge.

The components normal to the edge are built by the following formula,

$$F(\theta) = \frac{t_1 \cos\theta + t_2 \sin\theta}{\|t_1 \cos\theta + t_2 \sin\theta\|} \tag{6}$$

where the parameter θ is controlled by

$$\theta \in \begin{cases} \left[\dfrac{\pi}{2}, 2\pi\right] & \text{if} \quad t_1 \bullet t_1 + t_1 \bullet t_2 > 0 \\ & \text{and} \\ \left[0, \dfrac{\pi}{2}\right] & \text{otherwise} \quad t_2 \bullet t_2 + t_1 \bullet t_2 > 0 \end{cases} \tag{7}$$

and the vectors t_1 and t_2 are normal to e and contained in the faces adjacent to the edge. Then the ray directions can be computed as,

$$D(\theta) = \left\| v - \frac{e \bullet v}{\|e\|^2} e \right\| F(\theta) + \frac{e \bullet v}{\|e\|^2} e . \tag{8}$$

Observe that by sweeping θ over the range of values specified in equation (7), a family of diffracted patches is generated for the incident patch. The diffracted wave power levels are then assigned to each point using UTD [5] or a similar approximation [6], and the diffracted wave topology is assembled using the topology induced by $D(\theta)$.

V. INSTRUMENTATION

One of the most attractive features of ray models is that the impulse response of the channel is easy to compute [1]. From this, useful parameters such as the RMS delay spread can be extracted to yield predictions of coverage. The ray tracing, ray launching, and the wavefront launching methods sample the impulse response at given locations in space. The impulse response data contains wavefront arrival time, direction, and power density. The arrival direction allows the user to explore the use of directional antennas to cure multipath problems.

VI. RESULTS

A. Discussion of Images

Figure 3 shows the results of this model on a two room geometry. Despite appearances, the model is three dimensional. There is a single source, which appears near the center of the left room. This source emits a uniformly distributed spherical wavefront, and so is a simple model of an acoustic source or a electrically small antenna. Each of the walls is perfectly reflective, and there is a 3 dB attenuating window in the middle of the hallway. The plots on the left side of the figure are peak power density plots, and those on the right are RMS delay spread. The left plots indicate the signal strength of the dominant path. The RMS delay spread plots give an indication of multipath.
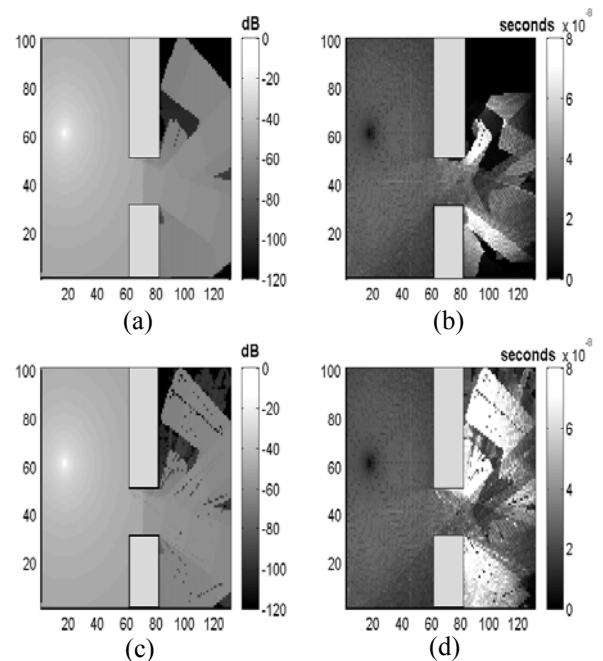

Fig. 3. (a) Relative power density (dB) without diffraction, (b) RMS delay spread (s) without diffraction, and (c) Relative power density (dB) with diffraction, (d) RMS delay spread (s) with diffraction.

The simulation was stopped after most of the signal had entered the right room, but before it reflected too many times. One can still see the wavefront structure in the upper half of the right room. It is evident that the diffracted waves contribute strongly to the multipath situation in the shadowed region of the right room. A strong diffracted wave reaches into the shadowed region well before the specular components from the incident wave. This results in a large delay spread, and would be problematic for wideband digital communications. Near the transmitter, the coherence bandwidth is roughly 16 MHz. In the shadowed region, the coherence bandwidth drops to 6 MHz, which represents a 266 % loss in available bandwidth.

B. Discretization Problems

The wavefront method avoids most discretization problems associated with ray launching, since it interpolates the wavefront between points on the wavefront set. However, discretization becomes evident when using a diffraction model, since diffracting edges cut apart incident wavefronts. If the wavefront is not sampled with enough points, these cuts will become jagged. This leaves gaps between the diffracted wavefront and the incident wavefront, which result in lost impulse response data. Some of these gaps can be seen in the lower plots of Fig. 3, where they look a little like streaky noise. The best solution for this problem is to resample incident wavefronts along a diffracting edge so that the cuts do not become jagged.

VII. FUTURE WORK

A. Ray Resampling

Like all numerical solvers for the wave equation, the wavefront model loses accuracy after a long period of simulation. This occurs when adjacent points become quite far apart. The wavefront set gradually becomes poorly sampled, and interpolating points on it is likely to be inaccurate. It seems that this problem could be alleviated by interpolating new points and rays onto the surface of the wavefront as time elapses. This would help avoid the discretization that appears in the diffraction results, and would also yield more accurate power density calculations.

B. Vector-Wave Models

The model presented here is a scalar model, which is assumed to be a good approximation of electromagnetic phenomena even though electromagnetic waves are polarized. The reflection and diffraction coefficients of many materials respond differently to waves of different polarization, so a vector wave formulation would allow the wavefront model to handle these sorts of materials.

VIII. CONCLUSIONS

Maintaining the topology of the wavefront allows for a simpler time-domain wave propagation model that is free from the problems associated with ray catching. Using interpolation over the surface of the wavefront, this model naturally incorporates diffracted waves and power density changes from beam spreading. The measurable quantities are automatically power densities, which do not need to be weighted by ray counts. It is also possible that this model can compensate for errors associated with discretization of the signal into rays, by carefully interpolating them over the wavefront. However, this particular aspect of the model has not been investigated.

REFERENCES

[1] H. R. Anderson, "A ray-tracing propagation model for digital broadcast systems in urban areas," *IEEE Transactions on Broadcasting*, vol. 39, no. 3, pp. 309–317, 1993.

[2] G. Durgin, N. Patwari, and T. S. Rappaport, "Improved 3d ray launching method for wireless propagation prediction," *Electronics Letters*, vol. 33, no. 16, pp. 1412–1413, 1997.

[3] L. C. Evans, *Partial Differential Equations*, American Mathematical Society, 1998.

[4] D. Chizhik, J. Ling, and R. A. Valenzuela, "The effect of electric field polarization on indoor propagation," *Proc. Int. Conf. Universal Personal Communications (ICUPC 98)*, Florence, Italy, pp. 459–462, 1998.

[5] T. W. Veruttipong, "Time domain version of the uniform GTD," *IEEE Transactions on Antennas and Propagation*, vol. 38, no. 11, pp. 1757–1764, Nov. 1990.

[6] G. Wölfle, R. Hoppe, T. Binzer, and F. M. Landstorfer, "Radio network planning and propagation models for urban and indoor wireless communication networks," *Millenium Conference on Antennas and Propagation (AP2000)*, Davos, Switzerland, April 2000.

Michael Robinson is a graduate student in the Center for Applied Mathematics at Cornell University, and also works part-time at Syracuse Research Corporation. He received his BS in Electrical Engineering and MS in Mathematics at Rensselaer Polytechnic Institute, in 2002 and 2003, respectively. His research interests involve using topological information to understand and simplify the solution of differential equations.